

## UNFROZEN WATER CONTENTS OF SUBMARINE PERMAFROST DETERMINED BY NUCLEAR MAGNETIC RESONANCE

ALLEN R. TICE<sup>1</sup>, DUWAYNE M. ANDERSON<sup>2</sup> and KAY F. STERRETT<sup>1</sup>

<sup>1</sup>*U.S. Army Cold Regions Research and Engineering Laboratory, Hanover, N.H., 03755 (U.S.A.)*

<sup>2</sup>*Faculty of Natural Sciences and Mathematics, State University of New York at Buffalo, Buffalo, N.Y., 14260 (U.S.A.)*

(Accepted for publication February 4, 1981)

### ABSTRACT

Tice, A.R., Anderson, D.M. and Sterrett, K.F., 1981. Unfrozen water contents of submarine permafrost determined by nuclear magnetic resonance. *Eng. Geol.*, 18: 135–146.

Prior work resulted in the development of techniques to measure the unfrozen water contents in frozen soils by nuclear magnetic resonance (NMR). It has been demonstrated that NMR is a promising new method for the determination of phase composition (the measurement of unfrozen water content as a function of temperature) which circumvents many of the limitations inherent in the adiabatic and isothermal calorimetric techniques. The NMR technique makes it possible, in a non-destructive, non-intrusive way, to explore hysteresis by determining both cooling and warming curves. Corrections are made for dissolved paramagnetic impurities which have the effect of increasing the signal intensity at decreasing temperatures. The results demonstrate that NMR techniques can be effectively utilized both at and below the melting point of ice in frozen soils and that accurate melting points (freezing point depressions) can be determined.

### INTRODUCTION

The recent construction of the Trans Alaska Oil Pipeline produced a new era in arctic construction. Thermopiles were installed in areas which took advantage of the cold Alaskan winters. By direct coupling the thermopiles cooled the underlying soil to somewhat lower temperatures than would be accomplished by natural convection. This undercooling insured that by the end of summer the soil would remain frozen and would thus provide a firm foundation for the vertical supporting members of the pipeline.

A knowledge of the thermal characteristics of the adjacent soil was required for effective thermopile design and operation. Of particular importance was a method to determine the phase composition of frozen soil, i.e., unfrozen water content versus temperature. The degree of sophistication required for the measurement of phase composition made in-situ field measurements impractical; therefore, indirect methods for deriving the amounts of unfrozen water were sought.

A basic relationship between the unfrozen water content and specific surface area can be traced back to Bouyoucos' early work (1917). Bouyoucos

presented data that showed major increases in the unfrozen water contents with decreasing particle sizes. Nersesova and Tsytoovich (1963) listed the specific surface area of the soil as one of the factors which governed the phase composition of soils. Next, Dillon and Andersland (1966) developed a useful prediction equation for unfrozen water content based on specific surface area, plasticity index and a defined activity ratio. Anderson and Tice (1973) reported that phase composition data could be well represented by a power curve:

$$W_u = \alpha \theta^\beta \quad (1)$$

where  $W_u$  is given in percentage dry sample weight,  $\theta$  is the temperature below zero in degrees C and  $\alpha$  and  $\beta$  are parameters characteristic of each soil. When the soil parameters  $\alpha$  and  $\beta$  are individually correlated with specific surface area determinations and combined with eq.1, the following equation is obtained (Anderson and Tice, 1972):

$$\ln W_u = 0.2618 + 0.5519 \ln S - 1.449 S^{-0.264} \ln \theta \quad (2)$$

From eq.2 it is possible to estimate the unfrozen water content at any temperature from a single measurement of a soil's specific surface area. This equation became a guide for the Alaskan Pipeline Company for thermal calculations of heat flow around thermopiles and drilling platforms. There are instances where prediction equations are not applicable. The equations take into consideration the unfrozen interfacial water associated with the mineral constituents only and do not account for any water which might exist between ice—grain boundaries. Also, if excessive solutes are present, a correction would have to be applied depending on the nature of the solutes present.

Tice et al. (1978a) recognized that the various calorimetric and dilatometric methods which were the standard procedures for determining unfrozen water contents in frozen soils would not readily adapt to field usage. They concentrated on a simplified technique which employed nuclear magnetic resonance (NMR). Although the results they reported agreed favorably with determinations made with the isothermal calorimeter, a refinement in both equipment and experimental procedure was needed. For instance, the NMR probe was cooled to the same test temperature as the samples. This resulted in detuning of the NMR probe and required an elaborate calibration procedure to compensate for temperature effects. Also, no correction was possible which compensated for the paramagnetic effect of the water and ions or the dependence of signal intensity on temperature.

Later, Tice et al. (1978b) eliminated most of the deficiencies inherent in their earlier investigation by employing a more sensitive NMR probe. The NMR probe was not cooled but was maintained at a uniform room temperature. The soil samples were instrumented with thermocouples and contained in a precision temperature bath. The fast response of the NMR analyzer allowed quick removal and replacement of the samples. Sequential readings were found to be proportional to sample unfrozen water content. Tice et al.

(1978b) corrected for the paramagnetic effect by using the last reading before spontaneous nucleation as a basis for the calculation of unfrozen water contents.

This report presents a refined method for determining the paramagnetic effect and explains how this effect influences the accuracy of unfrozen water content determinations by nuclear magnetic resonance. The total amount of unfrozen water for each sample was determined by differential scanning calorimetry and compared to values measured by NMR.

## MATERIALS AND METHODS

### *Location*

The materials used in this investigation were taken from two undisturbed sediment cores sampled from beneath the Beaufort Sea by Sellmann et al. (1976, 1977) during the 1976 and 1977 drilling program. Table I lists the sample location and other pertinent information.

### *Nuclear magnetic resonance*

Samples 1.6 cm in diameter by 4 cm length were removed from each core. A copper constantan thermocouple was inserted in the center of each specimen to monitor temperature. The soils were then sealed in glass test tubes with rubber stoppers to prevent moisture changes. The test tubes were immersed in a bath containing an ethylene glycol-water mixture. The temperature of the bath was controlled to within  $\pm 0.03^\circ\text{C}$  by a Bayley proportional-temperature controller.

A Praxis model PR-103 pulsed NMR analyzer was operated in the  $90^\circ$ -mode with a 0.1-sec clock, and at a fast scan speed. The first pulse amplitude in the  $90^\circ$ -mode was measured for each sample starting at  $+21.6^\circ\text{C}$ . The test tubes were sequentially removed from the bath, wiped dry and inserted in the NMR analyzer probe. After about 4 sec (the time required to record sample temperature and NMR amplitude), the samples were reinserted in the bath. When all samples had been analyzed, the bath temperature was lowered at  $3^\circ\text{C}$  increments and the measurements were repeated. Readings above the freezing point were used to determine the paramagnetic effect discussed in the next section. Around  $0^\circ\text{C}$  the temperature was lowered in smaller step-wise increments until the samples nucleated spontaneously. Complete cooling curves were obtained down to about  $-25^\circ\text{C}$ . The samples were then heated to obtain warming curves and to determine the melting points. Water contents were determined gravimetrically, and a ratio of the sample water content to projected first-pulse amplitudes was developed. Unfrozen water contents were calculated by multiplying first pulse amplitudes by their respective ratios to obtain a value for each temperature (Tice et al., 1978a, b).

TABLE I

Selected characteristics of three sediments from the Beaufort Sea

Sample No.* <sup>1</sup>	Location* <sup>1</sup>		Water depth* <sup>1</sup> (m)	Depth (m) below soil surface* <sup>1</sup>	Salinity* <sup>1</sup> (‰)	Calculated freezing point* <sup>2</sup> (°C)	NMR thawed data	
	Latitude	Longitude					A (eq.3)	B (eq.3)
PB-8-05	70° 28.5'N	148° 21.6'W	6.98	3.36	30.59	-1.62	654.408	-2.303
PB-8-12	70° 28.5'N	148° 21.6'W	6.98	7.67	31.07	-1.65	1096.341	-3.433
PB-2-8	70° 28.5'N	148° 18.1'W	11.6	8.44			652.009	-1.933

\*<sup>1</sup>Sellmann et al., 1976, 1977.\*<sup>2</sup>Page and Iskandar, 1978.

### *Differential scanning calorimetry*

Following the gravimetric water content determinations the soils were rewetted to their original water contents, sealed and allowed to stand one week for moisture equilibration. Aluminum sample pans and covers were weighed individually with a Perkin-Elmer thermogravimetric electro balance. Individual soil-water mixtures were compacted, leveled to the lip of the sample cup, sealed hermetically in a press, and then weighed. Each sample of the resulting soil-water-salt mixture weighed approximately 25 mg.

The samples were then individually placed in a Perkin-Elmer differential scanning calorimeter and cyclically frozen and melted 3 times at a scanning rate of  $80^{\circ}/\text{min}$ . Previously the calorimeter had been carefully calibrated for temperature and output by the measurement of spectral-grade standard samples of known weight. The melting points of chloroform ( $-63.5^{\circ}\text{C}$ ), dodecane ( $-9.6^{\circ}\text{C}$ ), benzene ( $+5.5^{\circ}\text{C}$ ) and indium ( $+156^{\circ}\text{C}$ ) served as temperature standards throughout the range of interest. During calibration runs, these fixed calibration temperatures were observed to fall within  $0.2^{\circ}\text{C}$  of the scanning calorimeter record. To determine the calibration for the measurement of phase transition energies in absolute terms, known amounts of spectral-grade indium were run. After the areas of the indium transitions were integrated, five separate determinations yielded an average heat of fusion of  $19.10 \text{ cal./g}$ . This value compared very favorably with the known heat of fusion of indium of  $19.16 \text{ cal./g}$ .

At the conclusion of the freeze-thaw cycling, each sample was allowed to equilibrate for 45 min to permit water redistribution within the sample. Following this, the samples were cycled at a programmed rate of  $5^{\circ}\text{C}/\text{min}$  at a calorimeter sensitivity of  $10 \text{ mcal/sec}$ . The phase transitions for both cooling and warming runs were recorded on a  $10''$ -strip chart recorder. At the conclusion of the calorimeter measurements, each sample was weighed to verify that no water had been lost during the measurements. Pinholes were punched in the sample covers and the samples were dried to a constant weight at  $110^{\circ}\text{C}$ .

Calculation of the total water frozen for each respective sample was accomplished by integrating the areas below the freezing peaks and comparing to the predetermined areas from the indium standard. By knowing the total sample water contents and assuming the standard heat of fusion for pure water, the total unfrozen water content for each respective sample was calculated.

### RESULTS AND DISCUSSION

Shown in Fig.1 is the effect of temperature on the NMR signal. When a temperature of about  $-4^{\circ}\text{C}$  was reached, spontaneous nucleation occurred which produced a sharp drop in signal intensity. The drop in signal intensity results from the fact that the NMR is tuned to the hydrogen proton associated with liquids. The signal associated with the solid ice and soil composition

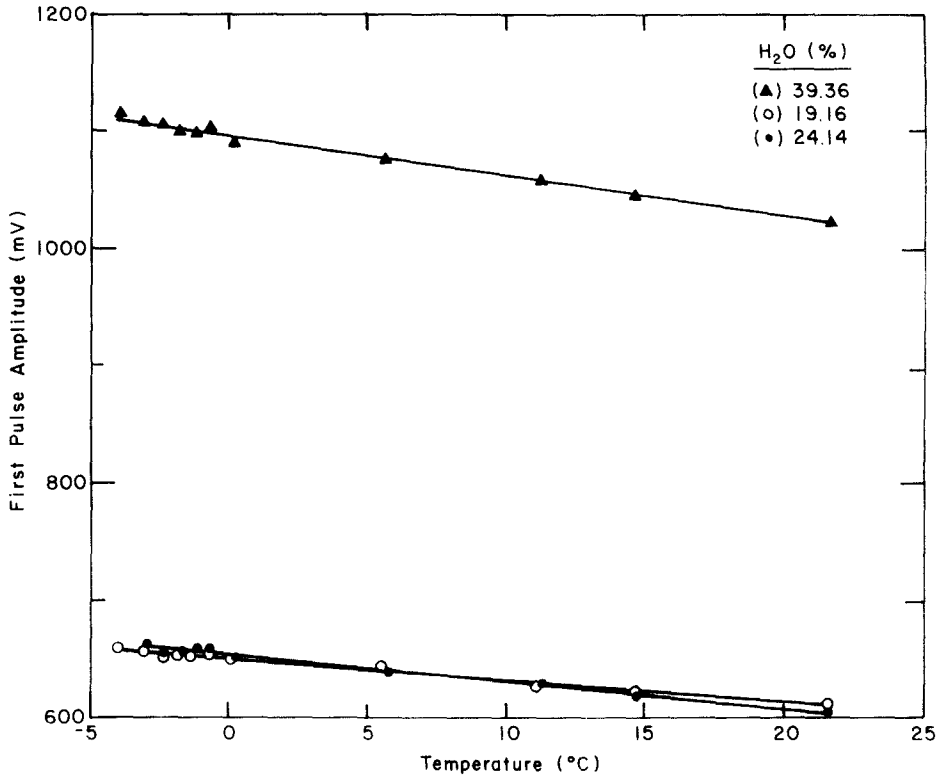


Fig.1. The effect of temperature on the signal amplitude.

protons are not recorded. If nucleation did not occur, however, a continuous linear relationship (i.e., without a sharp drop) between the signal intensity and temperature would be observed. The thawed experimental data (shown in Table I) are fitted by linear regression:

$$Y = A + BX \quad (3)$$

where  $A$  = intercept at  $0^{\circ}\text{C}$  and  $B$  = slope of the line.

The thawed values are projected beyond the point of spontaneous nucleation and at each individual temperature are utilized to calculate unfrozen water content by direct ratio (see Tables II–IV). Shown in these Tables are the experimental data for both cooling and warming runs. The NMR readings for the warming runs increase until the samples are melted. The calculated value of unfrozen water content for the first reading following total melt should be equal to the total gravimetric water content. In Tables II–IV the excellent agreement between these values is apparent.

Page and Iskandar (1978) reported many geochemical properties of the cores recovered from the Beaufort Sea drilling program. Using the ionic composition of the solutes present, they calculated freezing points at various depths for drill holes PB-5 through PB-9. According to their calculations, the

TABLE II

Unfrozen water content versus temperature of sediment sample PB-8-05

Temperature (° C)	Frozen NMR reading	Projected thawed NMR reading	Unfrozen water content (% dry weight)
-3.8	416	663	15.15
-4.2	376	664	13.67
-4.7	324	665	11.76
-5.3	301	667	10.89
-6.3	273	669	9.85
-6.9	254	670	9.15
-7.7	234	672	8.41
-8.8	216	675	7.73
-10.3	195	678	6.94
-12.0	168	682	5.95
-13.5	145	685	5.11
-16.3	122	692	4.26
-19.2	104	699	3.59
-22.2	95	706	3.25
-25.0	79	712	2.68
-22.3	89	706	3.04
-19.2	111	699	3.83
-16.4	126	692	4.40
-13.3	152	685	5.36
-10.3	183	678	6.52
-9.2	208	676	7.43
-8.1	219	673	7.86
-7.0	246	671	8.85
-6.0	272	668	9.83
-5.0	294	666	10.66
-4.4	336	665	12.20
-4.2	340	664	12.36
-4.0	362	664	13.16
-3.7	371	663	13.51
-3.5	384	663	13.98
-3.3	400	662	14.59
-3.1	420	662	15.32
-2.9	453	661	16.55
-2.7	475	661	17.35
-2.5	513	660	18.77
-2.3	562	660	20.56
-2.0	595	659	21.80
-1.9	622	658	22.82
-1.6	649	658	23.81 melted

Sample water content = 24.144

TABLE III

Unfrozen water content versus temperature of sediment sample PB-8-12

Temperature (°C)	Frozen NMR reading	Projected thawed NMR reading	Unfrozen water content (% dry weight)
-4.3	681	1111	24.12
-4.7	638	1112	22.58
-5.3	596	1114	21.06
-6.2	553	1118	19.47
-6.9	514	1120	18.06
-7.8	478	1123	16.75
-8.9	454	1127	15.85
-10.3	408	1132	14.18
-12.1	374	1138	12.93
-13.6	335	1143	11.53
-16.4	301	1153	10.27
-19.4	258	1163	8.73
-22.4	221	1173	7.41
-25.2	208	1183	6.92
-22.3	226	1173	7.58
-19.3	252	1163	8.53
-16.4	291	1153	9.93
-13.4	338	1142	11.65
-10.3	404	1132	14.05
-9.3	432	1129	15.06
-8.1	454	1124	15.90
-7.1	496	1121	17.41
-6.1	535	1117	18.85
-5.0	593	1113	20.97
-4.4	646	1111	22.88
-4.2	656	1111	23.24
-4.0	676	1110	23.97
-3.7	698	1109	24.77
-3.6	719	1109	25.52
-3.3	742	1108	26.36
-3.1	769	1107	27.34
-2.9	807	1106	28.72
-2.8	846	1106	30.10
-2.5	887	1105	31.59
-2.3	952	1104	33.94
-2.0	1016	1103	36.25
-1.9	1082	1103	38.61
-1.6	1104	1102	39.43 melted

Sample water content = 39.357

TABLE IV

Unfrozen water content versus temperature for sediment sample PB-2-8

Temperature (°C)	Frozen NMR reading	Projected thawed NMR reading	Unfrozen water content (% dry weight)
-4.3	526	660	15.27
-4.7	492	661	14.26
-5.3	460	662	13.32
-6.3	420	664	12.12
-6.9	387	665	11.15
-7.8	362	667	10.40
-8.8	338	669	9.68
-10.3	310	672	8.84
-11.9	288	675	8.18
-13.5	265	678	7.49
-16.3	239	684	6.70
-19.4	206	690	5.72
-22.4	191	695	5.27
-25.3	170	701	4.65
-22.3	187	695	5.16
-19.2	202	689	5.62
-16.3	220	684	6.16
-13.3	250	678	7.07
-10.2	297	672	8.47
-9.2	304	670	8.69
-8.1	333	668	9.55
-6.9	367	665	10.58
-6.0	393	664	11.34
-5.0	432	662	12.51
-4.4	466	661	13.51
-4.2	481	660	13.97
-3.9	500	660	14.52
-3.6	513	659	14.92
-3.5	532	659	15.47
-3.3	551	658	16.05
-3.1	562	658	16.37
-2.9	580	658	16.89
-2.7	604	657	17.62
-2.4	629	657	18.35
-2.2	656	656	19.16 melted

Sample water content = 19.165

freezing point for hole PB-8 at 3.36 and 7.67 m depths should average  $-1.63^{\circ}\text{C}$  (Table I). Our warming data (Tables II, III) show that at a temperature of  $-1.9^{\circ}\text{C}$  the samples are still partially frozen. Following the determinations at  $-1.9^{\circ}\text{C}$ , our next test temperatures of  $-1.6^{\circ}\text{C}$  show that the samples from this location are completely melted, which agrees well with the calculations of Page and Iskandar (1978); thus, if the temperature were raised in smaller increments, the NMR could also conveniently be used to determine

melting points of soil–water mixtures. Complete ionic composition data are not available for drill hole PB-2; however, the NMR data show that the sample is completely melted at a temperature of  $-2.2^{\circ}\text{C}$  (Table IV). This indicates a much higher salinity content than the samples from hole PB-8.

Unfrozen water content versus temperature curves are presented in Fig.2 for both cooling and warming runs. The data show that, hysteresis effects between cooling and warming determinations can readily be observed utilizing NMR, and that measurements at both low and high temperatures are easily obtainable.

Figure 2 shows that the unfrozen water contents of the two samples from drill hole PB-8 vary greatly even though the salt content is similar. This difference is due to the differences in sample water content and also textural variations that occur within the core. Page and Iskandar [10] report that PB-8-05 is classified as sandy-clay-silt (water content 24.14% in Fig.1) whereas PB-8-12 is a clayey silt, (water content 39.36%, Fig.1). Earlier, Tice et al. (1978b) reported that the unfrozen water contents vary directly with total sample water content for identical soils.

Figure 2 also shows that the unfrozen water content for sample PB-2-8 is higher than PB-8-5 even though the water content is lower. This is probably

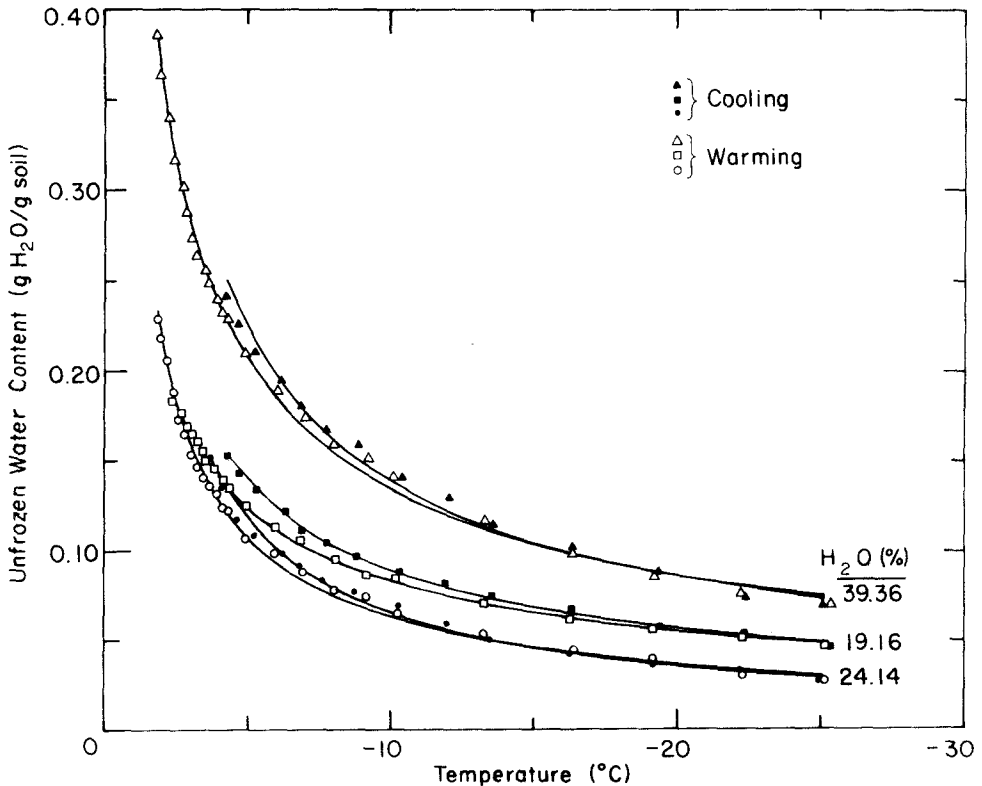


Fig.2. Unfrozen water content vs. temperature curves for three Beaufort Sea sediment samples.

due to the higher salinity content which is indicated by the much lower melting point. Contained in Table V is a comparison between unfrozen water content measurements which consider paramagnetic effects and those which are calculated from the last thawed reading prior to freezing. The data show no major differences throughout the temperature range of interest. It remains to be seen, however, what the result might be if high surface area clays containing large amounts of salts are analysed.

The results of the differential scanning calorimeter (DSC) runs which measured the total amount of unfrozen water are shown in Table VI. When these determinations are compared to the NMR data at the same temperatures, good correlations are observed. As previously mentioned in this paper, the DSC measurements were made on remolded and rewetted samples.

## CONCLUSIONS

This investigation again has demonstrated the utility of employing nuclear magnetic resonance (NMR) for the determination of unfrozen water content and melting point of frozen soil. The reproducibility of the NMR measurements near the melting point is reflected by the fact that the first measurements following melt is nearly equal to the sample water content. At the

TABLE V

Unfrozen water contents corrected and uncorrected for paramagnetic effects

Sample No.	Temperature (°C)	$W_u$ (% dry weight) corrected for paramagnetic effects	$W_u$ (% dry weight) uncorrected for paramagnetic effects
PB-8-05	-5.3	10.89	10.99
	-16.3	4.26	4.46
	-25.0	2.68	2.88
PB-8-12	-5.3	21.06	21.28
	-16.4	10.27	10.75
	-25.2	6.92	7.43
PB-2-8	-5.3	13.32	13.44
	-16.3	6.70	6.98
	-25.3	4.65	4.97

TABLE VI

Comparison between unfrozen water contents measured by differential scanning calorimetry (MDSC) and nuclear magnetic resonance (NMR)

Sample No.	Temperature (°C)	$W_u$ (DSC)	$W_u$ (NMR)
PB-8-05	-16.2	4.64	4.31
PB-8-12	-16.9	8.78	9.62
PB-2-8	-21.76	6.23	5.26

low temperature end, the measurements agree well with measurements by differential scanning calorimetry. The NMR technique is ideally suited to determine hysteresis between cooling and warming curves.

A method has been presented which can be used to correct for sample paramagnetic impurities. However, the data show that for the samples analyzed in this study, the paramagnetic effect does not influence the measurements of unfrozen water to a significant degree.

#### REFERENCES

- Anderson, D.M. and Tice, A.R., 1972. Predicting unfrozen water contents in frozen soils from surface area measurements. *Highway Res. Rec.*, 373: 12-18.
- Anderson, D.M. and Tice, A.R., 1973. The unfrozen interfacial phase in frozen soil water systems. In: *Ecological Studies*, 4. Springer, New York, N.Y., pp.107-124.
- Bouyoucos, G.J., 1917. Classification and measurement of the different forms of water in soils by means of the Dilatometer Method. *Mich. Agric. Exp. Stn., Tech. Bull.*, 36: 43 pp.
- Dillon, H.B. and Andersland, O.B., 1966. Predicting unfrozen water contents in frozen soils. *Can. Geotech. J.*, 3 (2): 53-60.
- Nersesova, Z.A. and Tsytoich, N.A., 1963. Unfrozen water in frozen soils. *Proc. Permafrost Int. Conf.*, NAS-NRC Publ. 1287: 230-234.
- Page, F.W. and Iskandar, I.K., 1978. Geochemistry of subsea permafrost at Prudhoe Bay, Alaska. *CRREL Spec. Rep.*, 78-14: 70 pp.
- Sellmann, P.V., Lewellen, R.I. Ueda, H.T., Chamberlain, E. and Blouin, S.E., 1976. USACRREL—USGS Subsea Permafrost Program, Beaufort Sea, Alaska. *CRREL Spec. Rep.*, 76-12: 20 pp.
- Sellmann, P.V., Chamberlain, E., Ueda, H.T., Blouin, S.E., Garfield, D. and Lewellen, R.I., 1977. *CRREL—USGS Subsea Permafrost Program Beaufort Sea, Alaska. CRREL Spec. Rep.*, 77-41: 19 pp.
- Tice, A.R., Burrous, C.M. and Anderson, D.M., 1978a. Determination of unfrozen water in frozen soil by pulsed nuclear magnetic resonance. *Third Int. Conf. on Permafrost*, pp.149-155.
- Tice, A.R., Burrous, C.M. and Anderson, D.M., 1978b. Phase composition measurements on soils at very high water contents by the pulsed Nuclear Magnetic Resonance technique. *Transport. Res. Rec.*, 675: 11-14.